



## Intrinsic kinetics study of LPDME process from syngas over bi-functional catalyst

G.R. Moradi\*, J. Ahmadpour, F. Yaripour

Catalysis Research Center, Department of Chemical Engineering, Faculty of Engineering, Razi University, Tagh Boostan, Kermanshah, Iran

### ARTICLE INFO

#### Article history:

Received 20 August 2007

Received in revised form 18 April 2008

Accepted 13 May 2008

#### Keywords:

Dimethyl ether

Syngas

Bi-functional catalyst

Slurry reactor

Kinetics model

### ABSTRACT

The intrinsic kinetics of the three-phase dimethyl ether (DME) synthesis from syngas over a bi-functional catalyst has been investigated in a agitated slurry reactor at 20–50 bar, 200–240 °C and H<sub>2</sub>/CO feed ratio from 1 to 2. The bi-functional catalyst was prepared by physical mixing of CuO/ZnO/Al<sub>2</sub>O<sub>3</sub> as methanol synthesis catalyst and H-ZSM-5 as methanol dehydration catalyst. The three reactions including methanol synthesis from CO and H<sub>2</sub>, methanol dehydration and water gas shift reaction were chosen as the independent reactions. A kinetic model for the combined methanol and DME synthesis based on a methanol synthesis model proposed by Graaf et al. [G.H. Graaf, E.J. Stamhuis, A.A.C.M. Beenackers, Kinetics of low pressure methanol synthesis, Chem. Eng. Sci. 43 (12) (1988) 3185; G.H. Graaf, E.J. Stamhuis, A.A.C.M. Beenackers, Kinetics of the three-phase methanol synthesis, Chem. Eng. Sci. 43 (8) (1988) 2161] and a methanol dehydration model by Bercic and Levec [G. Bercic, J. Levec, Intrinsic and global reaction rate of methanol dehydration over  $\gamma$ -Al<sub>2</sub>O<sub>3</sub> pellets, Ind. Eng. Chem. Res. 31 (1992) 399–434] has been fitted our experimental data. The obtained coefficients in equations follow the Arrhenius and the Van't Hoff relations. The calculated apparent activation energy of methanol synthesis reaction and methanol dehydration reaction are 115 kJ/mol and 82 kJ/mol, respectively. Also, the effects of different parameters on the reactor performance have been investigated based on the presented kinetic model.

© 2008 Elsevier B.V. All rights reserved.

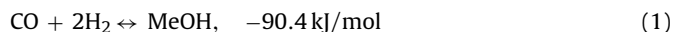
### 1. Introduction

Synthesis of new liquid fuel or other chemicals from coal or natural gas is becoming a hot research topic in many countries in recent years. Among those products, dimethyl ether (DME) is not only a clean fuel substituting for car and liquid petroleum gas (LPG) but also an excellent propellant and refrigerant. It is an important feedstock for the preparation of light alkenes too [1,2].

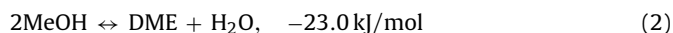
At present, DME is commercially prepared by dehydration of methanol using acidic porous catalysts such as zeolites, silica–alumina, alumina, etc. Recently, an original technique named STD (synthesis gas to dimethyl ether) process was developed for direct synthesis of DME from synthesis gas in a single reactor over a bi-functional catalyst [3]. The most common bi-functional catalysts reported in the literature for STD process are the physical mixture of the methanol synthesis catalyst and the solid acid catalyst [4]. Among the solid acids used for methanol dehydration, H-ZSM-5 and  $\gamma$ -Al<sub>2</sub>O<sub>3</sub> are the two catalysts that have been studied intensively

both for academic and commercial purposes [5]. Haldor-Topsoe has developed a bi-functional catalyst by the addition of H-ZSM-5 to the traditional CuO/ZnO/Al<sub>2</sub>O<sub>3</sub> methanol synthesis catalyst [6,7]. H-ZSM-5 is the best dehydration catalyst in STD process because of having a larger number of brønsted acid sites with moderate acid strength [8–10]. The main reactions in the STD process can be shown as follows [11]:

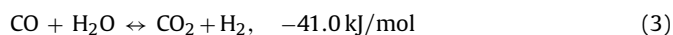
Methanol synthesis:



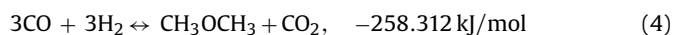
Methanol dehydration:



Water gas shift:



Overall reaction:



Methanol synthesis from synthesis gas is thermodynamically unfavorable, and thus high pressure is required for the reaction. Methanol is converted to DME by dehydration of methanol (Eq.

\* Corresponding author at: Catalysis Research Center, Department of Chemical Engineering, Faculty of Engineering, Razi University, Tagh Boostan, Kermanshah, Iran. Tel.: +98 8314274535; fax: +98 8314274542.

E-mail addresses: [gmoradi@razi.ac.ir](mailto:gmoradi@razi.ac.ir), [moradi.m@yahoo.com](mailto:moradi.m@yahoo.com) (G.R. Moradi).

(2) on the acid catalysts. Then, the equilibrium conversion shifts toward the right-hand side of reaction (1) [12]. The combination of these reactions results in a synergistic effect relieving the unfavorable thermodynamics for methanol synthesis: methanol, product in the first step, is consumed for reaction to dimethyl ether and water. The water is shifted by the WGS reaction (3) forming carbon dioxide and hydrogen, the latter being a reactant for the methanol synthesis. Thus, one of the products of each step is a reactant for another. This creates a strong driving force for the overall reaction allowing very high syngas conversion in one single pass [13].

The research of direct DME synthesis is focused on the catalyst and the process at present, but in order to provide basic data for designing the reactor for plant or industry, the kinetics study of direct DME synthesis from syngas is necessary. Furthermore, most of the kinetic studies reported in the literature for direct synthesis of DME were performed in fixed bed reactors because of their simplicity. However, better and more reliable kinetic data are available from tests made in slurry stirred tank reactors because of good temperature control that enables experiments at near isothermal conditions regardless of reaction heats and rates. Also, small catalyst particles can be used to eliminate intraparticle mass transfer effects in these reactors. Slurry stirred tank reactors have come to common use for methanol and dimethyl ether synthesis studies [2,14].

Ng et al. [2] investigated some key process variables which influence the reaction kinetics of the dual catalytic methanol and DME synthesis process in an internal recycle reactor. Zhouguang et al. [1] presented the intrinsic kinetics based on Langmuir–Hinshelwood mechanism for DME synthesis from syngas over a bi-functional catalyst mixed by methanol synthesis catalyst and methanol dehydration catalyst in a fixed bed reactor. Du et al. [15] also obtained the mechanism model in the fixed bed reactor.

A few literatures have been published for the kinetics of the liquid-phase dimethyl ether synthesis from syngas. Brown et al. obtained respective power function model. Peng et al. [14] studied the role each reaction plays in the synergy using kinetic simulations based on the power law form equations in slurry phase autoclave reactors. Guo et al. [16] investigated the global slurry kinetics based

on reasonable assumption and simplifications in a three-phase agitated reactor.

In all of these studies, the bi-functional catalyst consisted of a mixture of commercial Cu based methanol synthesis catalyst and a  $\gamma$ -alumina as the dehydration catalyst. But there is not any kinetic study based on Langmuir–Hinshelwood mechanism on a CuO–ZnO–Al<sub>2</sub>O<sub>3</sub>/H-ZSM-5 in LPDME process.

The present study, investigates the steady-state kinetics of single step DME synthesis on a CuO–ZnO–Al<sub>2</sub>O<sub>3</sub>/H-ZSM-5 catalyst in the slurry reactor. A kinetic model for this process based on proposed model by Graaf et al. [17,18] for methanol synthesis and methanol dehydration model by Bercic and Levec [19] has been developed. Moreover, the influences of different process parameters, such as pressure, temperature, H<sub>2</sub>/CO ratio in feed gas are simulated by the proposed kinetic models.

## 2. Experimental

### 2.1. Catalyst

Bi-functional catalyst (BFC) was prepared by admixing of the two catalysts, commercial methanol synthesis catalyst (manufactured by KMT Co.) and methanol dehydration catalyst (supplied by Süd-Chemie Co., sample no. 304H/06), namely H-ZSM-5. Two commercial catalysts were finely milled and sieved to sizes less than 90  $\mu\text{m}$ , and well mixed at mass ratio 3:1. This mass ratio obtained in our previous study [10]. Then the mixture was moulded under pressure into tablets, which were then crushed and sieved to 90–120 mesh size particles in order to avoid pore diffusional limitations. The description in detail about characterization test of the catalyst such as TPR, XRD, XRF and BET could be found elsewhere [20].

### 2.2. Experimental set-up and catalytic tests

A schematic view of the lab scale setup is shown in Fig. 1. In the feed section, the reactants CO and H<sub>2</sub> and nitrogen as the internal standard were fed through a set of mass flow controllers (Brooks 5850E & 5850S). After passage through mass flow controllers, the

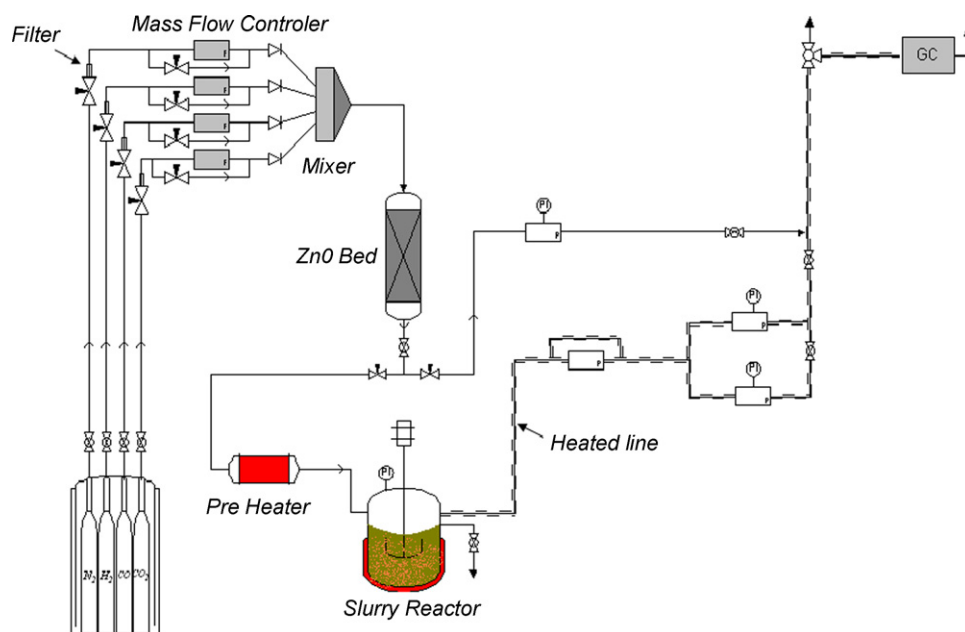


Fig. 1. Schematic view of the laboratory scale reactor system.

three gases were blended. Blended gases from mixer were passed over ZnO guard to remove any trace poisons, such as metal carbonyls. The mixture was preheated to the reaction temperature before entering the reactor. There was a backpressure regulator after the reactor. The down line effluent was constantly kept at temperatures over 100 °C, to avoid possible condensation of water or methanol, though their concentrations are very small after the reactions.

The STD reaction kinetic study was carried out in a 1 L mechanically agitated slurry reactor, equipped with a baffle and four bladed impeller, and withstanding temperatures up to 300 °C and pressures of 100 bar, in which the 10.5 g catalyst was suspended in 350 g liquid paraffin (treated to remove any trace poisons before use) with boiling point of higher than 305 °C.

Before each kinetic test, the catalysts had been reduced with pure hydrogen at the normal pressure according the following heating program: heated from room temperature to 250 °C with heating rate 1 °C/min and was kept for 6 h at this temperature. Then the catalysts were cooled to room temperature at the presence of hydrogen flow. After this pre-treatment, the feed (H<sub>2</sub>:CO:N<sub>2</sub>) was introduced into the slurry reactor. A small portion of the reactor effluent was sent to gas chromatograph (GC) for on line analysis. Varian CP-3800 gas chromatograph equipped with two packed columns: HaySep Q (80–100 mesh, 2 m × 1/8" × 2.0 mm, SS), Chrompach Molecular Sieve 13X (80–100 mesh, 2 m × 1/8" × 2.0 mm, SS) for separating CO<sub>2</sub>, H<sub>2</sub>, N<sub>2</sub>, CO & MeOH, DME, CH<sub>4</sub> respectively and detecting by a thermal conductivity detector (TCD). Analysis of water content in exit stream showed that H<sub>2</sub>O content was so small that it could not be detected. Then it was assumed that water-gas shift reaction in LPDME process is in equilibrium, because Cu-based methanol synthesis catalyst is really a good catalyst for water-gas shift reaction. Similar assumption was made by other researchers [16,21]. The water partial pressure is calculated by following equation:

$$P_w = \frac{P_{CO_2} P_{H_2}}{P_{CO} K_{p,WGS}} \quad (5)$$

where  $P_w$ ,  $P_{CO_2}$ ,  $P_{H_2}$  and  $P_{CO}$  are partial pressure (bar) of H<sub>2</sub>O, CO<sub>2</sub>, H<sub>2</sub> and CO, respectively; and  $K_{p,WGS}$  is the equilibrium constant of water-gas shift reaction.

### 2.3. Experimental condition

The kinetic experiments were always carried out under steady-state condition. This state was achieved within 20 h from start up. Mass and heat transfer limitations were negligible during the experimental conditions chosen. At a 3 wt% slurry (corresponding to 10.5 g of catalyst per 350 g of solvent) in a mechanically agitated slurry reactor, the gas solid mass transfer was not limit the overall rate. Also, in preliminary experiment it was checked for the intraparticle mass transfer limitation: above 1500 rpm of impeller speed, no mass transfer resistances were found. To assure that gas–liquid mass transfer limitations were absent, the experimental was carried out at 1600 rpm.

In order to carry out kinetic modeling, a broad range of experimental conditions have been carried out under the following reaction conditions: 200–240 °C, 20–50 bar, H<sub>2</sub>/CO molar ratio from 1:1 to 2:1 and space velocity of 1100 mLn/(g-cat h) which was sufficiently far from equilibrium conditions [20]. For each experiment the carbon balances over the reactor were calculated. The deviations were very small, usually less than 3%.

### 3. Simulation and parameter estimation

In the LPDME process, the real driving force for reactants should be the reactant concentration in liquid. But because of the absence

of mass transfer resistance as the control step, it may be assumed that the gas phase and the liquid phase to be in thermodynamic equilibrium. Then it would be logical to base the kinetic rate expression on fugacity of components. The fugacity of each component was calculated by SHBWR equation of state. Calculation showed that the difference between the reaction fugacity and the corresponding partial pressure of each component was very small.

Several kinetic models for methanol synthesis and methanol dehydration have been presented in literature, from the screening results of the other researcher, the model for methanol synthesis proposed by Graaf et al. [17,18] based on dual-site Langmuir–Hinshelwood mechanism (on site 1 CO and CO<sub>2</sub> adsorb competitively, while on site 2 H<sub>2</sub> and H<sub>2</sub>O adsorb competitively), and the dehydration model proposed by Bercic and Levec [19] based on reaction of dissociatively adsorbed methanol, were selected for analysis and simulation of the STD process. The kinetic rate equations for methanol synthesis and dehydration are Eqs. (6) and (7):

$$r_{CO,hydrogenation} : r_{M+2D} = \frac{k_1 K_{CO} [f_{CO} f_{H_2}^{3/2} - f_{CH_3OH} / (f_{H_2}^{1/2} K_{f_{CO}})]}{(1 + K_{CO} f_{CO} + K_{CO_2} f_{CO_2}) [f_{H_2}^{1/2} + (K_{H_2O} / K_{H_2}^{1/2}) f_{H_2O}]}$$
 (6)

$$r_{MeOH,dehydration} : r_D = \frac{k_2 K_M^2 (C_M^2 - C_W C_D / K_{f_{DME}})}{(1 + 2(K_M C_M)^{1/2} + K_W C_W)^4}$$
 (7)

where  $r_{CO,hydrogenation}$  is methanol equivalent productivity, the sum of methanol productivity and two time of DME productivity ( $r_{M+2D}$ ), and  $r_{MeOH,dehydration}$  is DME productivity ( $r_D$ ). The equilibrium constants for the three reactions ( $K_{f_i}$ ) given by Wang et al. [22]:

$$\log K_{f_{CO}} = 13.8144 + \frac{3748.7}{T} - 9.2833 \log(T) + 3.1475 \times 10^{-3} T - 4.2613 \times 10^{-7} T^2$$
 (8)

$$\log K_{f_{WGS}} = \frac{2167}{T} - 0.5194 \log T + 1.037 \times 10^{-3} T - 2.33 \times 10^{-7} T^2 - 1.2777$$
 (9)

$$\ln K_{f_{DME}} = \frac{4019}{T} + 3.707 \ln T - 2.783 \times 10^{-3} T + 3.8 \times 10^{-7} T^2 - 6.561 \times 10^4 T^2 - 26.64$$
 (10)

In the simulation of dimethyl ether synthesis reaction was assumed that the slurry reactor with excellent stirring operated as an ideal CSTR model. Justification of this assumption has been given by the other researchers [16,18,23].

Because of the reactor was backmixed, so the rate of formation or disappearance for the various species could be calculated directly from the inlet and outlet compositions and flow rates. So the experimental methanol equivalent productivity and DME productivity were calculated by the following equations:

$$r_{M+2D} = \frac{F_{out} \times (y_{MeOH} + 2y_{DME})}{W}$$
 (11)

$$r_D = \frac{F_{out} \times 2y_{DME}}{W}$$
 (12)

With knowing that nitrogen was not participate in any reactions of the STD process, the outlet flow rate obtained from N<sub>2</sub> balance:

$$F_{in} \times y_{N_2,in} = F_{out} \times y_{N_2,out}$$
 (13)

In the range of operating conditions employed in this work a total of 27 of experiments, contain individual and simultaneously effects of temperatures, pressures and feed compositions, were performed and used in the parameters optimization of Eqs. (6) and (7). Parameter optimization was based on the minimization of the following objective function:

$$OF = \sum_{i=1}^N w_i (r_i^{EXP} - r_i^{CAL})^2 \quad (14)$$

where  $N$  is the total number of experiments and  $w_i$  stands for the weight factor for response  $i$ . The latter was set proportional to  $1/r_i^{EXP}$ , because relative experimental errors are approximately the same for all experimental points over whole range of experimental conditions. Minimization of this objective function made use of simplex method [22].

## 4. Results and discussion

### 4.1. Kinetic parameters

Three sets of kinetic parameters were obtained for three different temperatures (200, 220, 240°C). To establish the kinetic parameters as a function of temperature, the following equation was used:

$$k_i(T) = A_i \exp\left(-\frac{B_i}{RT}\right) \quad (15)$$

where  $k_i$  denotes a model parameter,  $A_i$  is the pre-exponential factor, and  $B_i$  is the activation energy for a rate constant or heat of adsorption for adsorption equilibrium constant and then  $B_i < 0$ . By following the previously described methodology, the parameters of the proposed kinetics model, with a 95% confidence interval, are given by the following equations:

For methanol synthesis:

$$k_1 = 3 \times 10^8 \exp\left(-\frac{115656.054}{RT}\right) \quad (16)$$

$$K_{CO} = 2 \times 10^{-7} \exp\left(\frac{62030.754}{RT}\right) \quad (17)$$

$$K_{CO_2} = 6 \times 10^{-6} \exp\left(\frac{52276.7692}{RT}\right) \quad (18)$$

$$K_{H_2O}/K_{H_2}^{0.5} = 5 \times 10^{-13} \exp\left(\frac{115922.102}{RT}\right) \quad (19)$$

For methanol dehydration equation:

$$k_2 = 9 \times 10^6 \exp\left(-\frac{81051.5232}{RT}\right) \quad (20)$$

$$K_M = 0.6315 \exp\left(\frac{23304.142}{RT}\right) \quad (21)$$

$$K_W = 0.0014 \exp\left(\frac{37787.13}{RT}\right) \quad (22)$$

The Arrhenius plots for the rate constants are presented in Fig. 2, whereas the Van't Hoff relationships for equilibrium constants are shown in Figs. 3 and 4. Symbols represent the experimental results and lines model predictions. The good linearity confirms the validity of Eq. (15). Parity plots of the observed and calculated reaction rates for methanol synthesis and dehydration are presented in Figs. 5 and 6. Note that a majority of rate data lies in  $\pm 15\%$  region. These figures clearly show the excellent agreement between model calculations and experimental in whole range of operating conditions. It should be recalled that, in the calculations the equilibrium concentration of water was assumed.

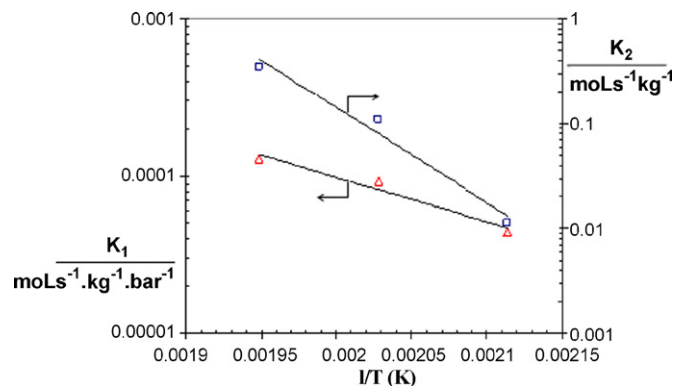


Fig. 2. Arrhenius plot for reaction rate constants: ( $\Delta$ )  $k_1$ , ( $\square$ )  $k_2$ . Symbols: regression per temperature. Lines: regression with all temperature.

According to these kinetic modeling results, the apparent activation energies for the direct DME synthesis from syngas on CuO–ZnO–Al<sub>2</sub>O<sub>3</sub>/H-ZSM-5 in slurry phase are derived from the slope of the straight lines of Arrhenius plot (Fig. 2) through linear fitting. Activation energy estimates of 115.66 and 81.05 kJ/mol are found for the methanol synthesis and dehydration reactions, respectively. These findings are in a good agreement with the results reported previously in the literature. Methanol synthesis activation energy reported 105.36 kJ for Graaf et al. kinetic model in the same conditions by Jinfu Wang et al. [23]. For methanol dehydration reaction, activation energy varies from catalyst to catalyst. As mentioned before most of kinetic studies have been done for  $\gamma$ -Alumina. For this catalyst, activation energy reported 105 kJ/mol for Bercic and Levec kinetic model by Chadwick [2]. Also, Jean Bandriera et al. report 80 kJ/mol on H-mordenite zeolite [24]. By comparing the kinetic behavior of the H-ZSM-5 zeolite with  $\gamma$ -Alumina in dual catalytic methanol and DME synthesis, our bi-functional catalyst is highly active in compare with the bi-functional catalyst that consists of  $\gamma$ -Alumina as dehydration part because of having a larger number of brønsted acid sites with moderate acid strength [8–11]. Furthermore, to evaluate the kinetic equations, material balances for any species  $i$  based on the CSTR reactor

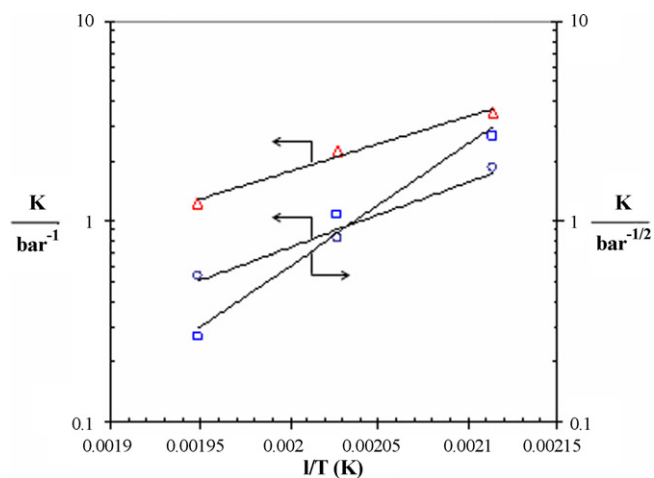
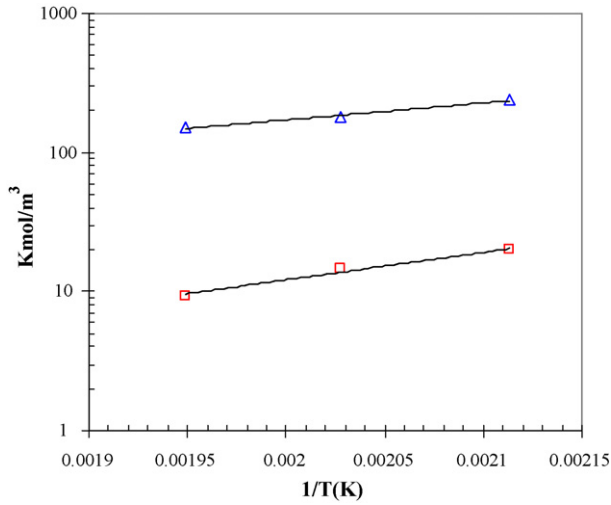


Fig. 3. Van't Hoff plot for adsorption equilibrium constants in methanol synthesis: ( $\circ$ )  $K_{CO}$ , ( $\Delta$ )  $K_{CO_2}$ , ( $\square$ )  $K_{H_2O}/K_{H_2}^{0.5}$ . Symbols: regression per temperature. Lines: regression with all temperature.



**Fig. 4.** Van't Hoff plot for adsorption equilibrium constants in methanol dehydration ( $\square$ )  $K_W$ , ( $\Delta$ )  $K_M$ . Symbols: regression per temperature. Lines: regression with all temperature.

are written [2]:

$$F_{in}Y_{i,in} - F_{out}Y_{i,out} = W \sum_j [v_{i,j}r_j] \quad (23)$$

The reaction rates,  $r_j$ , are given by the kinetic model described later. Solving balance equations for known kinetic expressions gives the outlet mole fractions of each component. Figs. 7–10 show the goodness of fitting between the experimental values and those calculated for the molar fraction of the main components.

#### 4.2. Dependence of kinetics of DME synthesis on the operating conditions

It is of interest to explore the dependence of kinetics of DME synthesis on the operating condition such as temperature, pressure and  $H_2/CO$  feed ratio. For the purposes of quantitative comparison with experimental result, the conversion of the feed carbon monoxide

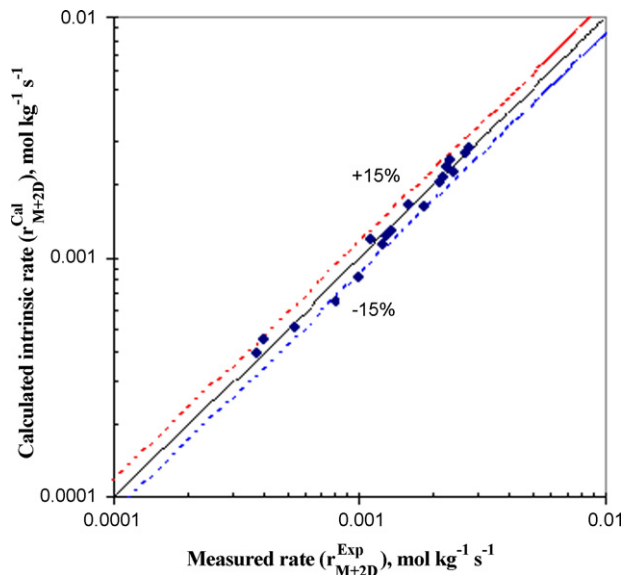


**Fig. 5.** Parity plot for the methanol synthesis reaction rate.

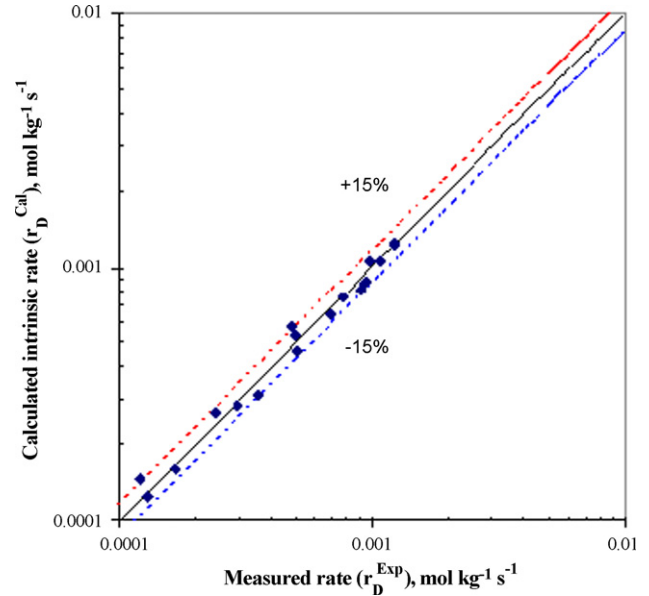


**Fig. 6.** Parity plot for the methanol dehydration reaction rate.

and yield of DME were used. These were defined as follows:

$$X_{CO} = \frac{F_{in}Y_{CO,in} - F_{out}Y_{CO,out}}{F_{in}Y_{CO,in}} \quad (24)$$

$$Y_{DME} = \frac{F_{out}Y_{DME,out}}{F_{in}Y_{CO,in}} \quad (25)$$

The measured results of  $X_{CO}$  and  $Y_{DME}$  in the range of operating conditions employed in this work are listed in Table 1.

##### 4.2.1. Effect of pressure

Fig. 11 shows the influence of pressure on the conversion of CO and yield of DME with both results of experimental (average values of 3 days time on stream) and simulation. As is observed, when pressure is increased in the range from 20 to 50 bar the conversion of CO increases, which is the logical consequence whereby

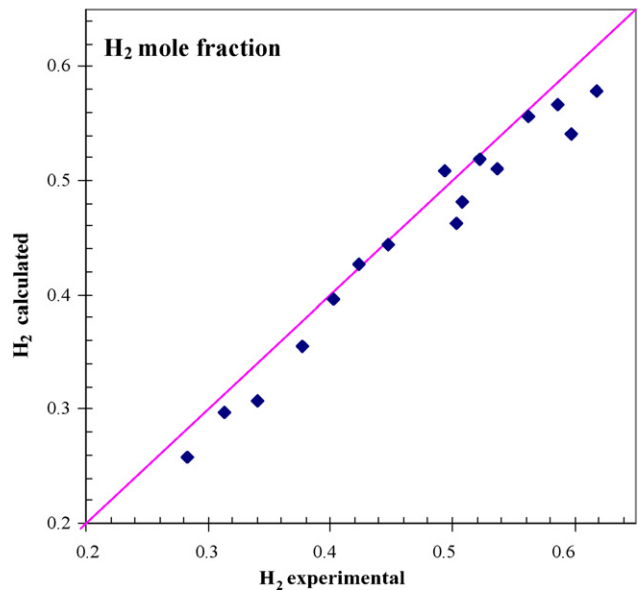


**Fig. 7.** Fitting between the experimental values of  $H_2$  molar fraction and the values calculated with kinetic model.



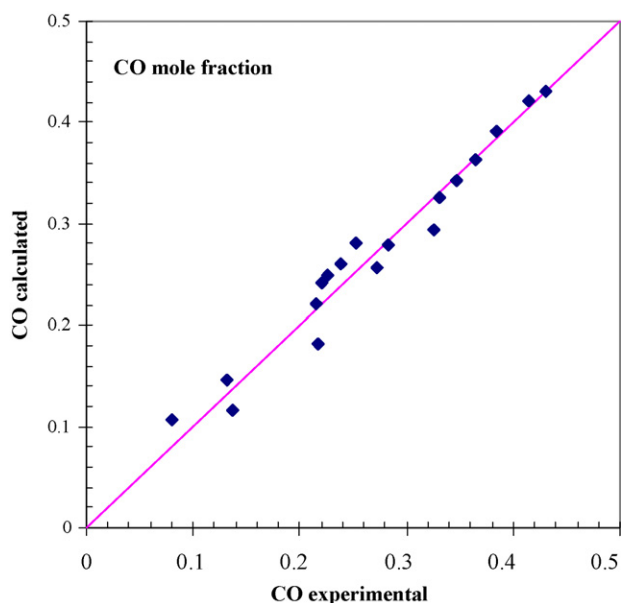


Fig. 8. Fitting between the experimental values of CO molar fraction and the values calculated with kinetic model.

methanol synthesis is the limiting step of the overall reaction. Also, methanol synthesis is a mole-number-reducing reaction so that pressure enhancement favors the conversion of CO and yield of DME. Since the number of moles in the both sides of methanol dehydration and water-gas shift reactions are the same, so the pressure has no effect on these reactions. This implies that the reaction of DME production may be carried out under a similar pressure as in the conventional synthesis of methanol [10,25,26].

#### 4.2.2. Effect of temperature

Fig. 12 shows the CO conversion and yield of DME as a function of reaction temperature. Results from simulation predict an increasing the CO conversion and DME yield as the temperature increases in the range of 200–240 °C, because the reactions rate are almost kinetically controlled in this region. The experimental results are in good agreement with the simulation. The reaction

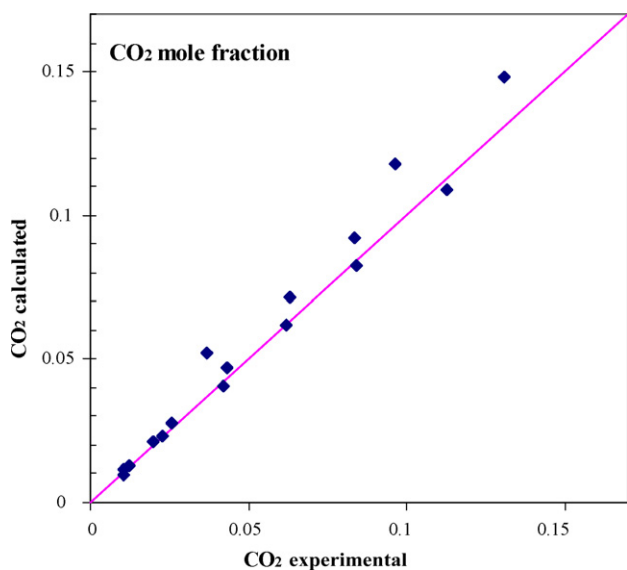


Fig. 9. Fitting between the experimental values of CO<sub>2</sub> molar fraction and the values calculated with kinetic model.

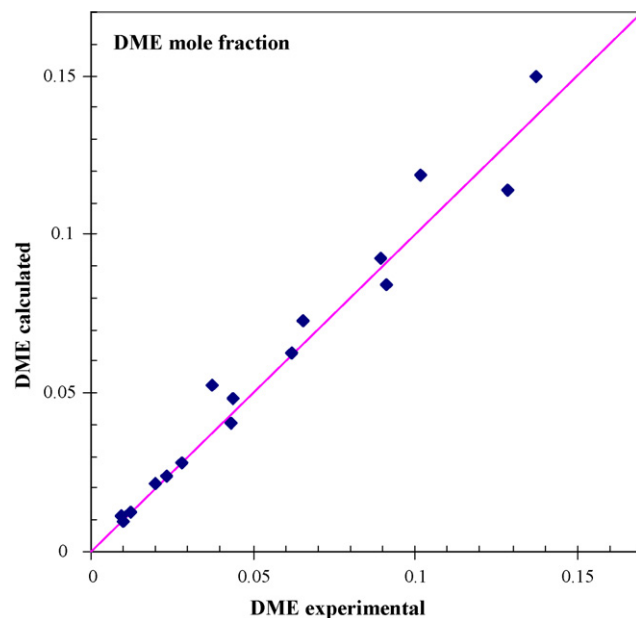


Fig. 10. Fitting between the experimental values of DME molar fraction and the values calculated with kinetic model.

rate is controlled by thermodynamic equilibrium at high temperatures, and thermodynamic influence becomes dominant in this case. Since methanol synthesis and methanol dehydration are both exothermic reactions, higher temperatures lead to an unfavorable effect on the equilibrium conversion of synthesis gas [27,28].

Table 1

The measured results of  $X_{CO}$  and  $Y_{DME}$  in the range of operating conditions employed in this work

$T$ (K)	$P$ (bar)	$H_2/CO$	$X_{CO}$ (mol%)	DME yield (mol%)
240	35	1.5	73.54	47.32
240	20	1.5	49.66	30.82
240	50	1.5	75.32	49.27
220	35	2	56.96	31.31
220	20	2	42.23	23.61
220	50	2	69.53	42.84
200	35	1	17.00	7.89
200	20	1	8.38	4.24
200	50	1	16.81	7.78
220	35	1.5	35.75	17.35
220	20	1.5	33.19	17.89
220	50	1.5	55.70	35.11
200	35	2	29.62	14.04
200	20	2	16.75	7.93
200	50	2	33.62	16.94
240	35	1	57.78	36.92
240	20	1	36.26	22.62
240	50	1	61.86	40.21
200	35	1.5	18.67	7.39
200	20	1.5	10.66	4.88
200	50	1.5	19.88	8.11
240	35	2	80.67	50.58
240	20	2	62.39	36.99
240	50	2	83.48	51.13
220	35	1	40.34	22.44
220	20	1	27.86	16.89
220	50	1	47.148	30.63

Reaction conditions:  $SV = 1100 \text{ mL}/(\text{g-cat h})$ , 1600 rpm, metallic to acidic function = 3/1 (wt./wt.%).

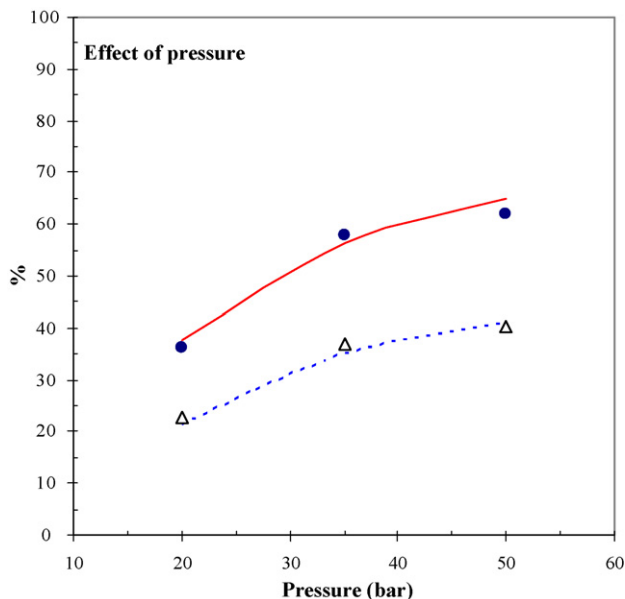


Fig. 11. Effect of pressure on simulation and experimental results:  $H_2/CO=1$ ,  $T=240^\circ\text{C}$ ,  $SV=1100\text{ mLn}/(\text{g-cat h})$ , (●)  $X_{CO}$ , (Δ)  $Y_{DME}$ ; Symbols: experimental, Lines: calculated.

#### 4.2.3. Effect of feed composition

Effect of feed composition ( $H_2/CO$  ratio) on the performance of STD process has been investigated. With increasing  $H_2/CO$  molar ratio, both CO conversion and DME yield increased. The experimental results are shown in Fig. 13 together with the results of simulation. An increase in the proportion of  $H_2$  in the reactant mixture favors CO conversion, which is the opposite of the case for the water gas shift reaction. The reaction order for the methanol synthesis reaction is (2), whilst for water gas shift the reaction order is 1 [22]. Furthermore, in the STD process, the conversion of CO is not dependent on the acidic property of the dehydration component, if the solid acid catalysts are so active for methanol dehydration that the intrinsic methanol synthesis rate is much lower than the

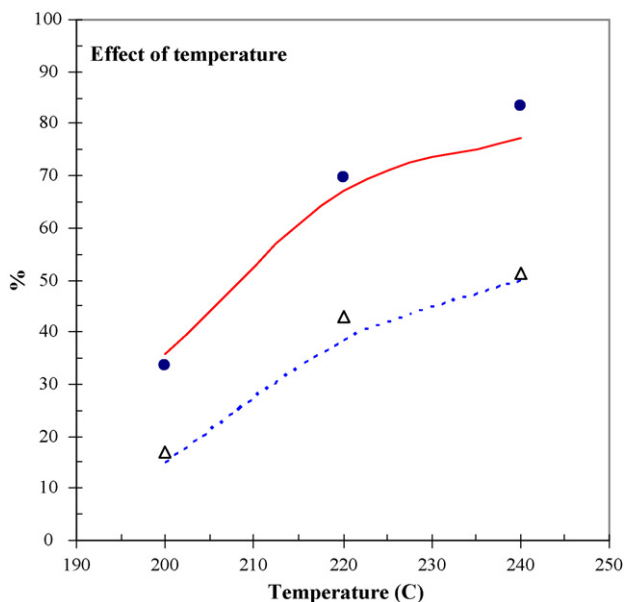


Fig. 12. Effect of temperature on simulation and experimental results:  $H_2/CO=2$ ,  $P=50\text{ bar}$ ,  $SV=1100\text{ mLn}/(\text{g-cat h})$ , (●)  $X_{CO}$ , (Δ)  $Y_{DME}$ ; Symbols: experimental, Lines: calculated.

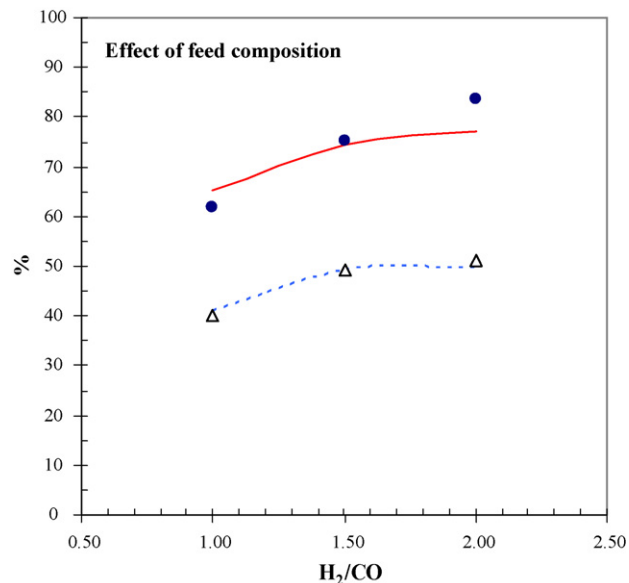


Fig. 13. Effect of  $H_2/CO$  in feed gas on simulation and experimental results:  $P=50\text{ bar}$ ,  $T=240^\circ\text{C}$ ,  $SV=1100\text{ mLn}/(\text{g-cat h})$ , (●)  $X_{CO}$ , (Δ)  $Y_{DME}$ ; Symbols: experimental, Line: calculated.

methanol dehydration rate [29]. Thus, with the increases of  $H_2/CO$  ratio, methanol synthesis reaction is accelerated, which lead to higher CO conversion and DME yield; because of methanol synthesis, is favored by  $H_2$  rich environment with the maximum rate at  $H_2/CO$  feed ratio of 2:1 [30,31].

## 5. Conclusions

A kinetic model for the LPDME process over a  $\text{CuO-ZnO-Al}_2\text{O}_3/\text{H-ZSM-5}$  catalyst based on a methanol synthesis model proposed by Graaf et al. [17,18] and a dehydration model by Bercic and Levec [19] was found to agree well with experimental results over a wide range of experimental conditions. The kinetic parameters were determined as function of the temperature between  $200^\circ\text{C}$  and  $240^\circ\text{C}$ . The performance of the syngas-to DME reaction system was determined by kinetics model. The calculated apparent activation energy of methanol synthesis reaction and methanol dehydration reaction are  $115.66\text{ kJ/mol}$  and  $81.05\text{ kJ/mol}$ , respectively. This accurate kinetic model based on LHHW approach can be used in future reactor modeling and scaling-up.

#### Notation

$A$	pre-exponential constant
$B$	activation energy or heat of adsorption ( $\text{J mol}^{-1}$ )
$C$	concentration ( $\text{kmol m}^{-3}$ )
$E$	activation energy ( $\text{J mol}^{-1}$ )
$f$	fugacity (bar)
$F$	molar flow rate ( $\text{mol s}^{-1}$ )
$k$	reaction rate constant
$K$	adsorption equilibrium constant
$K_f$	equilibrium constant
$N$	total number of experiments
$P$	pressure (bar)
$r$	reaction rate ( $\text{mol kg}^{-1}\text{ s}^{-1}$ )
$R$	gas constant ( $8.314\text{ J mol}^{-1}\text{ K}^{-1}$ )
$SV$	space velocity ( $\text{ml g}^{-1}\text{ h}^{-1}$ )
$T$	temperature (K)
$w$	the weigh sum of the squares

$W$	weight of catalyst (g)
$X_{CO}$	CO conversion
$y$	mole fraction
$Y_{DME}$	yield of DME

#### Greek symbols

$V_{ij}$	stoichiometric coefficient of component $i$ involved in chemical reaction $j$
----------	---

#### Superscripts

EXP	experimental value
CAL	calculated value

#### Subscripts

in	inlet of reactor
out	outlet of reactor

#### Acknowledgments

The authors acknowledge the financial support of this work by research and technology affairs of National Iranian Petrochemical Company.

#### References

- [1] Z Nie, H Liu, D. Liu, W. Ying, D. Fang, Intrinsic kinetics of dimethyl ether synthesis from syngas, *J. Nat. Gas Chem.* 14 (2005) 22–28.
- [2] K.L. Ng, D. Chadwick, B.A. Toseland, Kinetics and modelling of dimethyl ether synthesis from synthesis gas, *Chem. Eng. Sci.* 54 (1999) 3587.
- [3] D.M. Brown, B.L. Bhatt, T.H. Hsiung, J.J. Lewnard, F.J. Waller, Novel technology for the synthesis of dimethyl ether from syn gas, *Catal. Today* 8 (1991) 279–304.
- [4] J. Xia, D. Mao, B. Zhang, Q. Chen, Y. Tang, One-step synthesis of dimethyl ether from syngas with Fe-modified zeolite ZSM-5 as dehydration catalyst, *Catal. Lett.* 98 (4 (December)) (2004).
- [5] Y. Fu, T. Hong, J. Chen, A. Auroux, J. Shen, Surface acidity and the dehydration of methanol to dimethyl ether, *Thermochim. Acta* 434 (2005) 22–26.
- [6] Holder Topso, US Patent 4,536,485 (1993).
- [7] Holder Topso, US Patent 5,189,203 (1993).
- [8] T. Takeguchi, K. Yanagisawa, T. Inui, M. Inove, Effect of the property of solid acid upon syngas-to-dimethyl ether conversion on the hybrid catalysts composed of Cu–Zn–Ga and solid acids, *Appl. Catal. A: Gen.* 192 (2000) 201–209.
- [9] F. Yaripour, F. Baghaei, I. Schmidt, J. Perregaard, Catalyst dehydration of methanol to dimethyl ether (DME) over solid-acid catalysts, *Catal. Commun.* 6 (2005) 147–152.
- [10] G.R. Moradi, R. Ghanei, F. Yaripour, Determination of the optimum operating conditions for direct synthesis of dimethyl ether from syngas, *Int. J. Chem. Reactor Eng.* 5 (2007).
- [11] L. Wang, D. Fang, X. Huang, S. Zhang, Y. Qi, Z. Liu, Influence of reaction conditions on methanol synthesis and WGS reaction in the syngas-to-DME process, *J. Nat. Gas Chem.* 15 (2006) 38–44.
- [12] J.-H. Kim, M.J. Park, S.J. Kim, O.-S. Joo, K.-D. Jung, DME synthesis from synthesis gas on the admixed catalysts of Cu/ZnO/Al<sub>2</sub>O<sub>3</sub> and ZSM-5, *Appl. Catal. A: Gen.* 264 (2004) 37–41.
- [13] J.L. Li, X.G. Zhang, T. Inui, Improvement in the catalyst activity for direct synthesis of dimethyl ether from synthesis gas through enhancing the dispersion of CuO/ZnO/ $\gamma$ -Al<sub>2</sub>O<sub>3</sub> in hybrid catalysts, *Appl. Catal. A* 147 (1996) 23.
- [14] X.D. Peng, B.A. Toseland, P.J.A. Tijm, Kinetic understanding of the chemical synergy under LPDMETM conditions once-through applications, *Chem. Eng. Sci.* 54 (1999) 2787–2792.
- [15] M.X. Du, Y.W. Li, H.M. Huang, et al., Study on the process and kinetics of synthesis of methanol and dimethyl ether from CO + H<sub>2</sub>. Part II. Kinetic model, *Meitan Zhuanhua (Coal Conversion)* 6 (4) (1993) 68.
- [16] G. Junwang, N. Yuqin, Z. Bijiang, Global kinetic study of LPDME process from syngas, *J. Nat. Gas Chem.* 9 (4) (2000).
- [17] G.H. Graaf, E.J. Stamhuis, A.A.C.M. Beenackers, Kinetics of low pressure methanol synthesis, *Chem. Eng. Sci.* 43 (12) (1988) 3185.
- [18] G.H. Graaf, E.J. Stamhuis, A.A.C.M. Beenackers, Kinetics of the three phase methanol synthesis, *Chem. Eng. Sci.* 43 (8) (1988) 2161.
- [19] G. Bercic, J. Levec, Intrinsic and global reaction rate of methanol dehydration over  $\gamma$ -Al<sub>2</sub>O<sub>3</sub> pellets, *Ind. Eng. Chem. Res.* 31 (1992) 399–434.
- [20] G.R. Moradi, M. Nazari, F. Yaripour, Statistical analysis of the performance of a bi-functional catalyst under operating conditions of LPDME process, *Chem. Eng. J.* 140 (2008) 255–263.
- [21] M.R. Gogate, S. Lee, C.J. Kulik, A single-stage, liquid-phase dimethyl ether synthesis process from syngas. I. Dual catalytic activity and process feasibility, *Fuel Sci. Tech. Int.* 9 (6) (1991) 653–679.
- [22] W. Zhiliang, W. Jinfu, R. Fei, H. Minghan, J. Yong, Thermodynamics of the Single-Step Synthesis of Dimethyl Ether from Syngas, *Tsinghua Science and Technology*, pp. 168–176, ISSN 1007-0214 07/20.
- [23] M. Setinc, J. Levec, On the kinetics of liquid-phase methanol synthesis over commercial Cu/ZnO/Al<sub>2</sub>O<sub>3</sub> catalyst, *Chem. Eng. Sci.* 54 (1999) 3577–3586.
- [24] J. Bandiera, C. Naccache, Kinetics of methanol dehydration on dealuminated H-mordenite: model with acid and basic active centers, *Appl. Catal.* 69 (1991) 139–148.
- [25] J. Ereña, R. Garoña, J.M. Arandes, A.T. Aguayo, J. Bilbao, Effect of operating conditions on the synthesis of dimethyl ether over a CuO–ZnO–Al<sub>2</sub>O<sub>3</sub>/NaHZSM-5 bi-functional catalyst, *Catal. Today* 107–108 (2005) 467–473.
- [26] W. Zhiliang, D. Jie, W. Jinfu, Tsinghua, J. Yong, Study on synergy effect in dimethyl ether synthesis from syngas, *Chin. J. Chem. Eng.* 9 (4) (2001) 412–416.
- [27] K.-W. Jun, W.-J. Shen, K.-W. Lee, Concurrent producing of methanol and dimethyl ether from carbon dioxide hydrogenation: investigation of reactor condition, *Bull. Korean Chem. Soc.* 20 (9) (1999).
- [28] W. Zhiliang, D. Jie, W. Jinfu, J. Yong, Chin, The synergy effect of process coupling for dimethyl ether synthesis in slurry reactors, *Chem. Eng Technol.* 24 (2001) 5.
- [29] D. Mao, W. Yang, J. Xia, B. Zhang, Q. Song, Q. Chen, *J. Catal.* 230 (2005) 140–149.
- [30] W.-Z. Lu, L.-H. Teng, W.-D. Xiao, Simulation and experiment study of dimethyl ether synthesis from syngas in a fluidized-bed reactor, *Chem. Eng. Sci.* 59 (2004) 5455–5464.
- [31] W.-Z. Lu, L.-H. Teng, W.-D. Xiao, Theoretical analysis of fluidized-bed reactor for dimethyl ether synthesis from syngas, *Int. J. Chem. Reactor Eng.* 1 (2003), Note S2.